Journal of Engineering Science and Technology
Vol. 17, No. 5 (2022) 3187 - 3202

MODELING OF WIND TURBINE BASED ON GAUSSIAN PROCESSES

THAKER NAYL[1, 2]

[1]University of Information Technology and Communications,
College of Engineering, Baghdad, Iraq
[2]Lulea University of Technology, Department of Computer Sciences,
Electrical and Space Engineering, Lulea, Sweden
E-mail: thaker.nayl@ltu.se

Abstract

This paper proposes a realistic principal Gaussian Process model for the wind turbine, with a kernel derived. The model is trained and validated on a data-driven practical wind turbine model to predict optimal operational curves for the optimal operating conditions of wind turbine generators. The proposed technique indicates the critical parameters of the wind behaviour from historical wind speed data to keep maximum power. This technique is used to avoid periodic fluctuations in the output power of the wind turbine generators by design an efficient control system. The frequent changes in the power output come from tower shadow, wind shear, gust, and turbulence in the wind speed. The operational curves of the critical parameters included the profiles of power, blades pitch angle, and turbine rotor speed. The power improvement performance of the turbine can use the relationship between critical parameters ahead of time to predict wind behaviour.

Keywords: Blade pitch angle, Gaussian process, Tower Shadow, Wind shear, Wind turbine generator.

1. Introduction

Wind turbines can generate sustainable, clean, and affordable electrical power. Due to the stochastic and variable nature of the wind speed, the prediction unit requires a detailed analysis of the flow wind behaviour. An assortment of factors causes the fluctuation of the electrical power of wind turbines; some of them are predictable. In this case, it is essential to tackle the problem by expecting wind speed behaviour. An effective Gaussian Process (GP) regression will be applied to predict optimal operational curves of wind turbine generators.

A Gaussian Process is a non-parametric, nonlinear machine learning approach widely used in modelling complex and nonlinear systems [1]. Several regression methods for linear and nonlinear functions are obtainable in the fields of study using specific techniques. Stetco et al. [2] presented a review of machine learning methods for GP regression with supervised learning predicts an output variable using labelled input data.

There are many different types of learning algorithms presented in machine learning, such as series correlated data models and machine learning models [3]. The time series of models mainly include the moving average model, autoregressive model, and auto-regressive moving average model [4]. Due to the non-linearity of wind speed behaviour, the time series of models need data-stable assumptions [5].

Many machine learning methods are used to predict it, such as regression of GP to deal with the non-linearity of wind speed profile [6], support vector regression method [7], and quantile regression method that predicted wind speed [8]. Also, Li and Shi [9] and Manobelet al. [10] presented the wind speed forecasting using artificial neural networks presented a GP data pre-filtering method and artificial neural network model for predicting wind turbine power curves. Hoseinzadeh et al. [11] presented a comprehensive analysis of the effect of wind speed and angle on the wake development of an air-foil that works as wind turbine blades.

Finally, Strutz [12] used a nonlinear least square method is considered as a sub-optimal approach. The optimization problem of power energy is subjected to physical constraints [13]. Cai et al. 14] studied multi-task GP regression model to consolidate the numerical predictions of wind speed and Carrillo et al. [15] reviewed the modelling for wind turbine curve using a generic equation. All these manuscripts focused on the accuracy of wind speed predictions, and none consider the influence of tower shadow and wind shear effects.

The article's contribution is to develop a complete wind turbine model that includes wind shear and tower shadow parameters. These parameters highly influence the power output as a turbulence problem. For better prediction of the wind speed at different times field of view, the prognosis is made by different types of data-driven methods. In this article, the data-driven approach is proposed to predict wind behaviour from past wind speed data.

The outline of the article is as follows: Section II describes the problem formulation of the periodic fluctuations in the output power of the wind turbine. Section III presents the standard Gaussian Process Regression. Section IV describes operational curves of a wind turbine such as the power curve, blade pitch curve, and rotor curve. Section V includes the turbine model. Section VI proposes the

Gaussian Process approach for predicting the operational curves. Section VII presents the simulation analysis and evaluates the accomplishment of the GP operational curve models. Section VIII depicted concluding remarks.

2. Problem Formulation

The electrical power is exponentially proportional to wind speed, should do the wind speed study of any proposed site done accurately to ensure maximum power generation. The inconsistency of wind speed leads to periodic fluctuations in the output power. The factors that affect the inconsistent wind speed are tower shadow, wind shear, gust, and turbulence in the wind speed. The effect of tower shadow, wind shear and wind direction on the power output of wind turbines have been evaluated separately by Dolan and Lehn [16]. The equivalent wind speed v_{eq} that includes the effects from the base-line wind speed v_{bl} at hub height, the tower shadow v_{ts} and the wind shear v_{ws}, can be expressed in the following formula.

$$v_{eq} = v_{bl} + v_{ts} + v_{ws} \qquad \text{(1)}$$

It is noticed that the tower shadow, wind shear, and wind direction fluctuations varied the power producing capability. Figure 1 shows the horizontal axis wind turbine generator. The wind turbine under phenomena known as wind shear and tower shadow, which causes blades vibrations and power fluctuations. The wind speed sensation when the blades face the turbine tower during the rotation is called the tower shadow. Generally, wind speed at high altitudes is higher than at lower altitudes; this phenomenon is called wind shear. These phenomena cause periodic fluctuations in the power output that comes from tower shadow and wind shear.

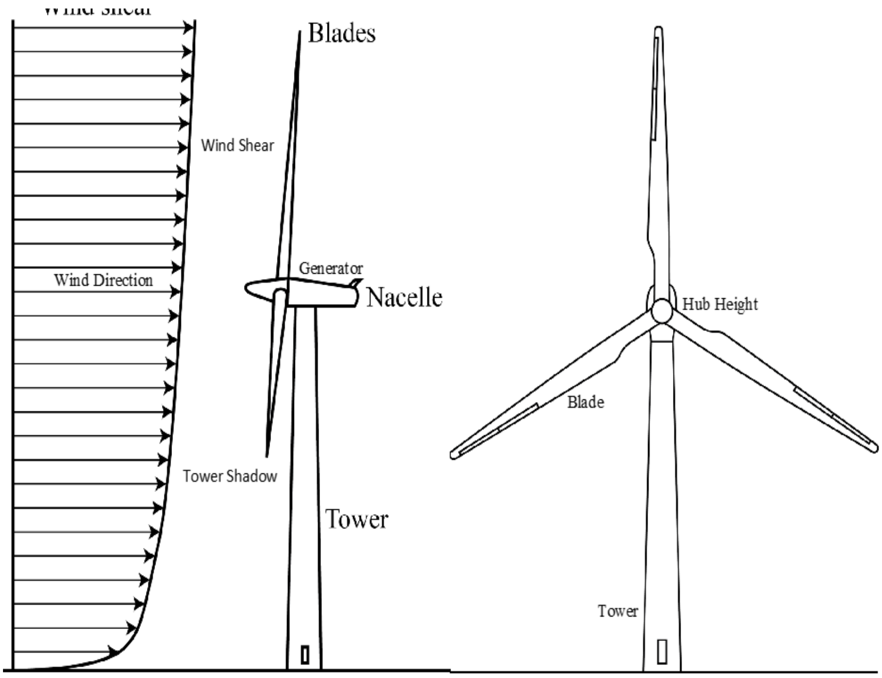

Fig. 1. Wind turbine under phenomena known as wind shear and tower shadow causes blades vibrations and power fluctuations.

Figure 2 shows these phenomena. Wind speed prediction is a significant challenge due to the periodic fluctuations in wind speed under complex environmental conditions.

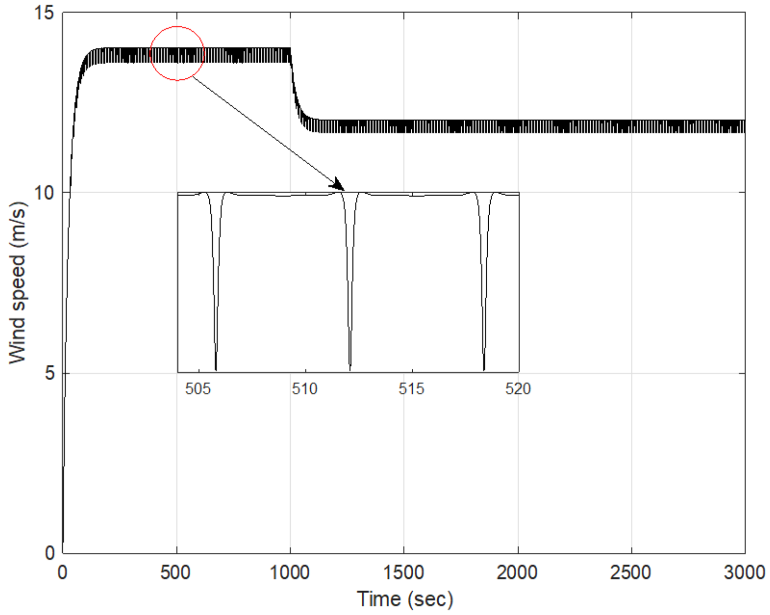

Fig. 2. Tower shadow and wind shear effects of wind turbine with tower radius (*r* = 10 m), and the distance from the blade to the tower (*x* = 5 m).

3. Standard Gaussian Processes Regression

A brief outline of GP regression will be discussing in this section. Regression is predicting the value of certain variables based on measurements of other variables. GP regression is about approximating a function $f(x)$, the measured the function $f(x_i)$ at a measurement training points x_i to predict the optimum values of $f(x_*)$. Consider the linear regression model of the form [16].

$$y_i = f(x_i) + \epsilon = x^T\, w + \epsilon \tag{2}$$

where the noise $\epsilon \sim \mathcal{N}(0, \sigma_n^2)$ is a zero mean and variance σ_n^2, can be predicted the coefficients w from a set of data by considering the standard deviation. The noiseless GP regression observes a training set of data.

$$f(x) \sim \mathcal{GP}(\mu(x), \kappa(x, x')) \tag{3}$$

where $\mu(x)$ is the mean value of the function $f(x)$, the $\kappa(x, x')$ is a covariance function for the vector (x, x') that is specified by a chosen kernel function.

We assumed that $f_* = f(x_*)$ is the prediction at x_*, x_* is a new point where the prediction is made, and the target outcomes y have a joint Gaussian distribution. To accomplish that, we can write it as follows,

$$\begin{bmatrix} y \\ f_* \end{bmatrix} \sim \mathcal{N}\left(\begin{bmatrix} \mu_1 \\ \mu_2 \end{bmatrix}, \begin{bmatrix} K + \sigma_n I & \kappa_*^T \\ \kappa_* & \kappa_{**} \end{bmatrix}\right) \tag{4}$$

For symbols convenience, the stenography $K = \kappa(X, X')$, $\kappa_* = \kappa(X, x_*)$, and $\kappa_{**} = \kappa(x_*, x_*)$, have been used, where X is the training dataset. For simplicity, we use the prior mean $(\mu_1, \mu_2) = 0$. The Radial-basis function is a stationary kernel. It is known as the squared exponential kernel, either a scalar or a vector with the same number of dimensions as the inputs x_i. The squared exponential kernel function is given by [17].

$$\kappa(x, x') = \sigma_f^2 \, exp\left(-\frac{(x - x')^2}{2\ell^2}\right) \tag{5}$$

where σ_f indicates the variance output signal and ℓ is a characteristic length scale.

The hyperparameters σ_f and ℓ can be selected under specific conditions. The effect of the kernel width parameter can be evaluated by choosing $\sigma_f^2 = 1$, and it is parameterized by a length scale parameter $\ell^2 > 0$. If we know f, then the prior distribution $p(f_*|x_*, X, y)$ letting us derive the predictive distribution analytically for the computational performance target, then the posterior distribution of f_*, the posterior mean μ_* and covariance σ_* can be calculated in the forms as follows.

$$p(f_*|x_*, X, y) \sim \mathcal{N}(\mu_*, \sigma_*) \tag{6}$$

$$\mu_* = k_*^T (K + \sigma_n^2 I)^{-1} \, y \tag{7}$$

$$\sigma_* = k_{**} - k_*^T (K + \sigma_n^2 I)^{-1} \, k_* \tag{8}$$

If the training set contains an observation of the function f_2, then the multivariate normal will give an updated prediction of f_2, as $p(f_1 \,|\, f_2)$, and we can write as follows [17].

$$p(y|X) = \left(\mu_1 + \frac{k_*^T}{k_{**}}(f_* - \mu_2)\right), \left((K + \sigma_n I) - \frac{k_* k_*^T}{k_{**}}\right) \tag{9}$$

The central equation of the GP regression function is in the simplest form as above. The algorithm learns by itself and can consider uncertainties of predicting the critical parameters.

4. Operational Curves of Wind Turbine

The performance of the wind turbine generators depends on the combination of the area of the rotor of the turbine, air density and wind speed. As a result of the aerodynamic torque, the wind turbine blades start to rotate, and this rotation leads to an angular velocity in the rotor side of the mechanical subsystem. Some strategies such as flow control techniques have been presented to increase the efficiency of variable speed wind turbines can be utilized in this subsystem [18].

It should be known for accurate modelling of wind turbine operation to guarantee power production running at maximum capacity. The power production of wind turbines also depends on the aerodynamic coefficient C_p. As referred to the Betz limit [19], the ultimate value of aerodynamic coefficient $C_p(\lambda, \beta)$ under ideal theoretical conditions is 0.593.

$$C_p(\lambda, \beta) = 4a(1 - a)^2 \tag{10}$$

where, a is the turbine axial induction coefficient, valid for ($0 \leq a \leq 0.5$).

The variation of the aerodynamic coefficient $C_p(\lambda, \beta)$ versus the blade pitch angle (β; [°]) and the tip speed ratio ($\lambda = \frac{wR}{v}$; [−]). The parameters such as rotor speed (w_r; [rps]), the radius of turbine hub (R; [m]), and the wind speed (v; [m/s]) are known. The rotor speed ($w_r = 2\pi f$), and (f; [rps]) is the frequency rotation of the turbine. The typical operating of the wind turbine will have to rotate at a fixed tip speed ratio. Figure 3 shows there is a unique optimal value of tip speed ratio λ that can satisfy maximum power coefficient $C_p(\lambda, \beta)$ under controlling blades pitch angle β. For higher wind speeds, the power in the wind continues to increase while $C_p(\lambda, \beta)$ starts to decrease. At rated wind speed and $\lambda \geq 2$, maximum capacity in the current depends on the maximum values of $C_p(\lambda, \beta)$. After that point, $C_p(\lambda, \beta)$ decreases, so power starts a slight decrease. The electrical power curve, blade pitch angles curve, and rotor speed curve will be demonstrated as a function of wind speed.

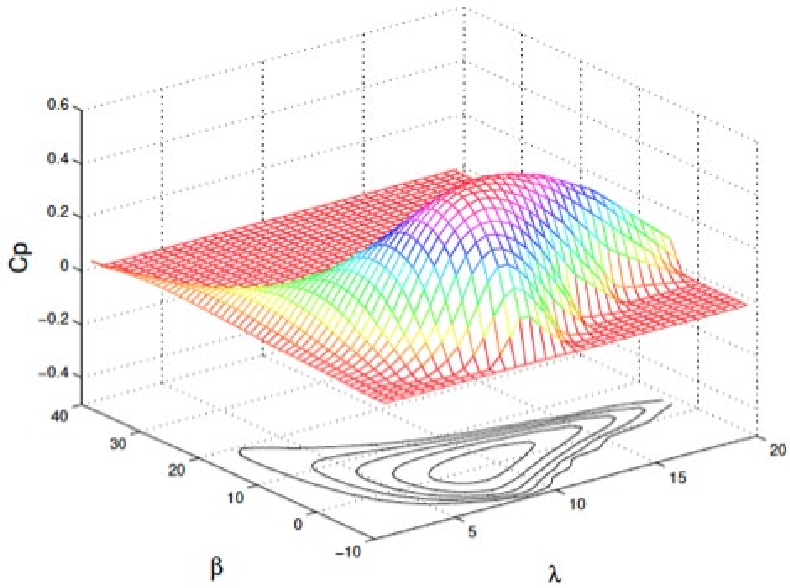

Fig. 3. Calculated $C_p(\lambda, \beta)$ surface.

4.1. Electrical power curve

Power production is a function of the wind speed, which describes the electrical power curve provided by the wind turbine manufacturer. The electrical power curve is a nonlinear relationship between output power and wind speed. The available active power is proportional to air density, wind speed, and its production depends on the swept area of the wind turbine. This relationship also depends on the aerodynamic power coefficient, which is extracted mathematically in [20].

$$P_e = 0.5\, \rho\, A\, v_{eq}^3\, C_p(\lambda, \beta) \tag{11}$$

where ρ is air density (kg/m^3), A is the swept area (m^2), v is the hub wind speed (m/s), and $C_p(\lambda, \beta)$ is the power coefficient of the wind turbine.

The maximum value of aerodynamic coefficient C_p under ideal theoretical conditions, which represents this variation of power output to the wind speed, is shown in Fig. 4. The simplification sets the C_p value constant at its maximum value for all wind speeds more significant than a particular value.

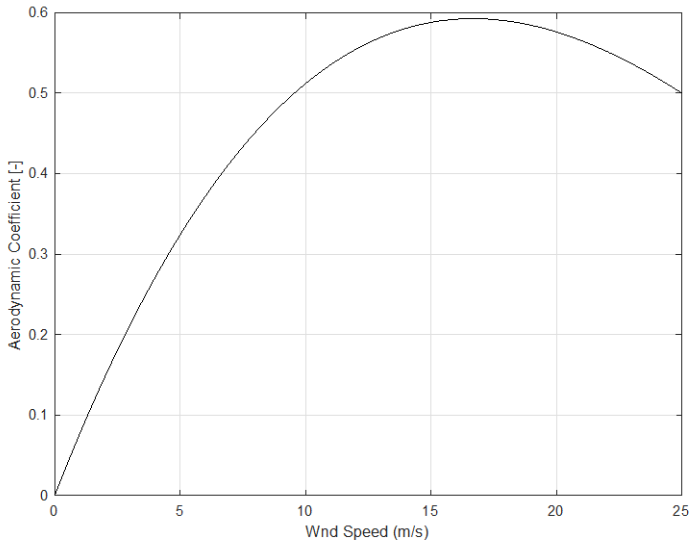

Fig. 4. The aerodynamic coefficient curve *Cp* with its associated wind speed.

4.2. Blade pitch angle curve

The curve of a blade pitch angle describes the relationship between the turbine pitch angle and the wind speed. The presence of small values of the blade pitch angle signifies a high value of wind speed. This relation is illustrated in Fig. 5. The pitch angle is adjusted to capture maximum power production during the rated wind speed (10<*v*<25) m/s.

4.3. Rotor speed curve

The rotor speed of the wind turbine and wind speed is called the rotor speed curve. The rotor curve is proportional to the wind speed and is found after a cut-in wind speed v_c when the wind speed, ($v_c > 5\ \mathrm{m/s}$). Figure 6 shows the relationship between the wind speed and the rotor shaft speed. The rated rotor speed is around ($w_r = 17\ \mathrm{m/s}$). These curves are worthy of implementing the maximum power generation, caused by predicting any difference from a typical rotor speed curve.

5. Turbine Model

The wind turbine considered here is always supposed to follow the wind direction. Therefore, we do not need to control the yaw angle of the turbine, which is used to rotate it into the wind. The wind turbine can extract enough power to accelerate itself at the desired operation angular velocity. The control strategy in this research is to control the rotor speed w_r of the wind turbine and the pitch angle of the blades β. This is generally done above cut-in wind speed v_c conditions when the wind speed ($v > 5\ \mathrm{m/s}$).

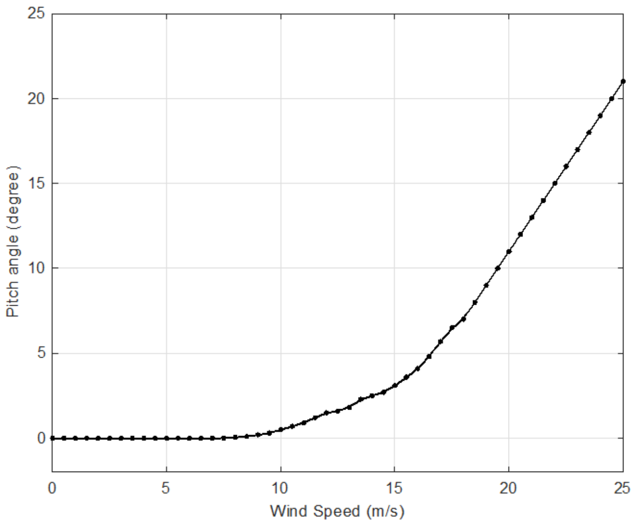

Fig. 5. Blade pitch angle curve vs wind speed.

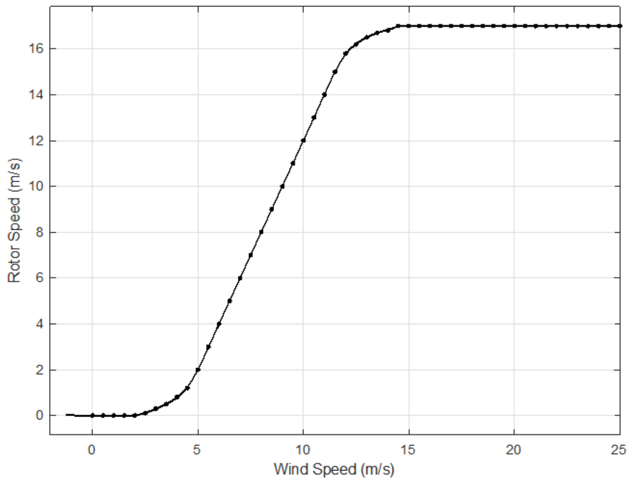

Fig. 6. Rotor speed curve vs wind speed.

At rated wind speed v_r conditions, it is common to control the pitch angle of the blades to keep the turbine rotor at a certain rated speed, which is done through full-span pitch actuator motors. When the wind speed exceeded the rated wind speed, the rotor speed of the turbine may exceed manufacturing limits. Hence the turbine should not be operated unloaded. The aerodynamic efficiency (C_p; [kgm^2]) is the ratio of instantaneous turbine power to wind power, can be defined as.

$$C_p(\lambda, \beta) = 0.5176(116\lambda_i - 0.4\beta - 5) * \exp(-21\lambda_i) \tag{12}$$

where the formula can calculate the coefficient λ_i,

$$\lambda_i = \frac{1}{\lambda + 0.08\beta} - \frac{0.035}{1+\beta^3} \tag{13}$$

The coefficient λ_i be contingent on the tip speed ratio λ and the blade pitch angle β. The dynamic behaviour of the pitch angle actuator, which is changed by a mechanical, hydraulic actuator, has been implemented in the scenario, which the equation can describe.

$$\dot{\beta} = -\frac{1}{\tau}\beta_a + \frac{1}{\tau}\beta_d \tag{14}$$

where the blade angle β tracks the desired blade angle β_d, and β_a is the actual pitch angle, and τ is the time constant of the actuator.

6. Proposed Approach

The GP state-space model can be formed as a transference function $f(x^k, u^k, \epsilon)$ is modelled as a GP model. The noise ϵ can be explained as the numerical uncertainty. A GP is parameterized by a mean function $\mu(x)$ and the squared exponential kernel function $\kappa(x, x')$ and mathematically, for the finite combination of data inputs x. The kernel function measures the similarity between two sets of data points to calculate the GP regression's closeness and core.

For the choice of $kernel$, the interactions between the velocity v_{eq} and the aerodynamic coefficient C_p need to be included. This is achieved by using a so-called additive kernel as follows [17].

$$\kappa(x, x') = \sigma_{\beta}^2\, exp\left(-\frac{(\beta-\beta')^2}{2\ell_{\beta}^2}\right) + \sigma_{w_r}^2\, exp\left(-\frac{(w_r-w_r')^2}{2\ell_{w_r}^2}\right) \tag{15}$$

where $(\sigma_\beta, \sigma_{w_r}, \ell_\beta, \ell_{w_r})$ represent the hyperparameters.

The vector of values of the function $f(x)$ in Eq. (3) is only one sample from a multivariate GP distribution equal to many measured coordinates of x. The prediction intervals and the predicted responses of the GP regression when the observations are noise-free, and the standard deviation is almost zero, as shown in Fig. 7. When observations include noise, as shown in Fig. 8, the feature GP regression applied to the wind speed with unknown amplitude, phase and mean.

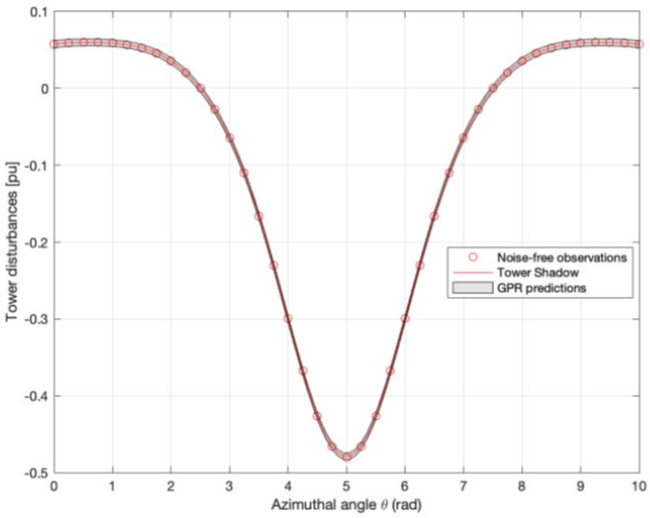

Fig. 7. The predicted responses of the GP regression fit when the observations are noisy and noise free.

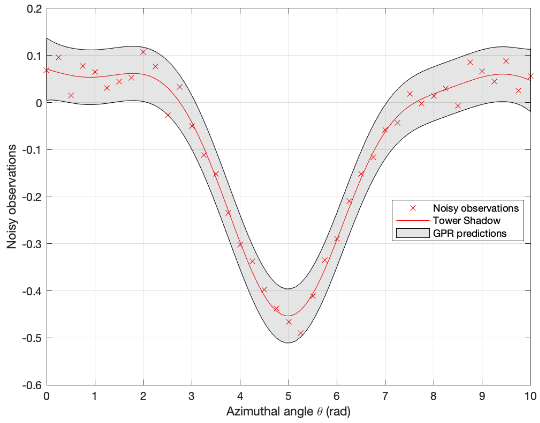

Fig. 8. The Gaussian process approximation fit of noisy observations and two standard deviations plotted as shaded area.

7. Simulation Results

The GP process included inverting a matrix process with many samplings data makes the modelling inaccurate, complex, and time-consuming. The wind data sets were selected from a monitoring station in the National Institute of Wind energy [21].

In this study, the only data available is wind speed, and a zero mean function will be assumed with Gaussian characteristics. The specifications of the wind turbine that we considered in this research is as follows: R = 38 m, w = 17 rps, β= (0-90)°, $\dot{\beta} = \mp 5^{\circ}$, $v_c > 5$ m/s, $v_r = 12$ m/s, and $\rho = 1.025$ kg/m^3.

The long-term monitoring of wind speed is shown in Fig. 9. The figure shows the random variation of the wind speed. The data sets can be downloaded as an excel file at a sampling time of 10 minutes per point. Figure 10 shows a small number of the data sets for 500 sampling times. There are 4000 observations in the training data set and 500 observations in the test data set, which is randomly selected from the testing data set.

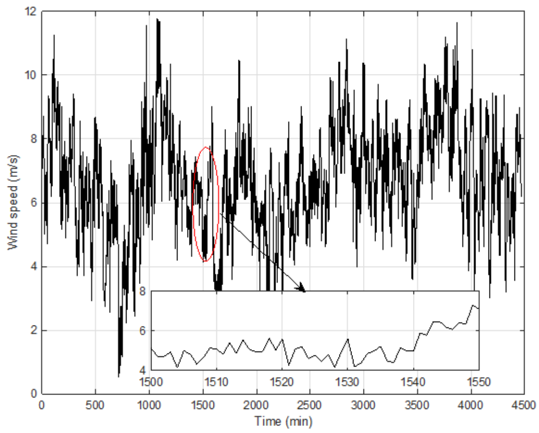

Fig. 9. The real data wind speed profile with sampling time 10 min.

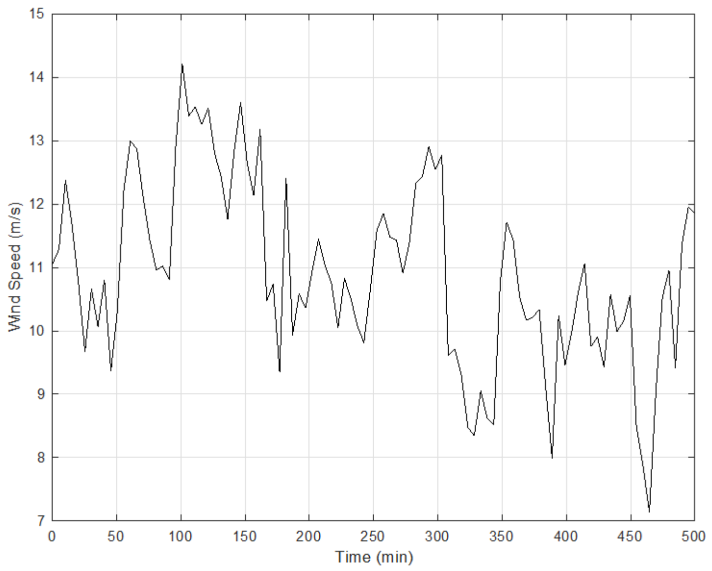

Fig. 10. The wind speed profile for 500 sample time.

Fit a GP regression using the kernel function with a short length scale for each predictor. The GP regression is used to enhance the efficiency of wind turbine power production, to predict wind speed, including tower shadow and wind shear prediction, which is considered the contribution of this article. The GP model is implemented in MATLAB for finding the hyperparameters.

The simulation is summarized in the below algorithm.

ALGORITHM

- Define wind turbine parameters.
- Input: training data x, training data y, test data x*
- Output: prediction interval
- Fit RGP models to the observed data sets.
- Exact fitting and prediction method.
- Compute the predicted responses and prediction intervals using the fitted models.

We consider the training set in the array and fit GP models to the observed data sets. Use the exact fitting and prediction methods.

Finally, the predicted responses and prediction intervals using the fitted models have been computed. A small number of samplings data makes the modelling accurate. The power output of the turbine is an important characteristic which represents the performance of the system. Figure 11 shows the results of GP, where the predicted upper and the lower bound and the average values are given. GP carefully follows the expected variance values of the wind speed.

The expected variance is (0.65) and the time elapsed is 0.1425 seconds. The wind speed shows the periodic fluctuation behaviour. Therefore, it is appropriate to use the v_{eq} formula containing periodic fluctuation to predict wind speed. Figure 12 shows the results of the turbine's power output and its GP prediction, with noise-free observation. The predicted responses of the GP regression fit the observations. The standard deviation of the predicted response is minimal, which is between (0-0.02).

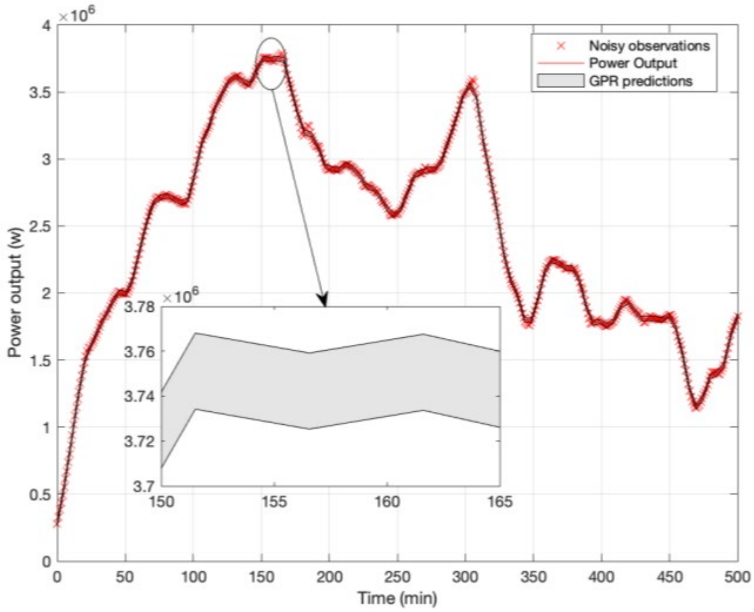

Fig. 11. The Wind speed with GP regression fit of noisy observations and the two standard deviations plotted as shaded area.

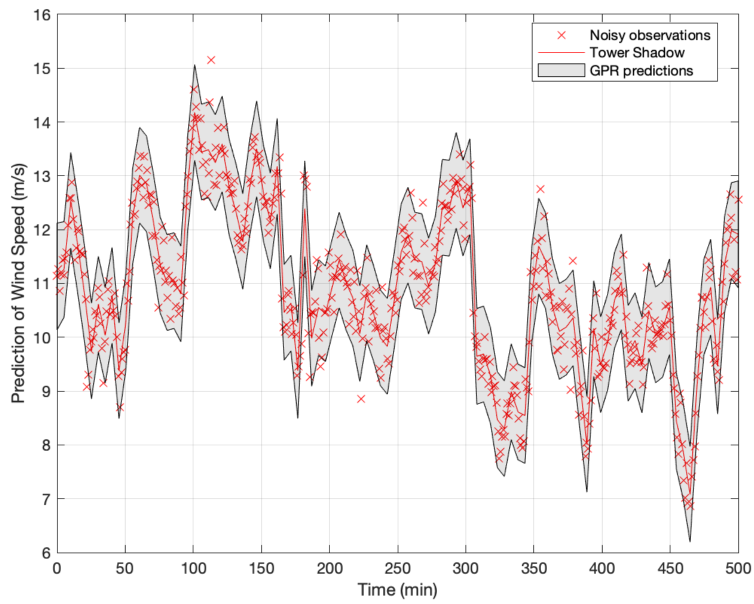

Fig. 12. The power output of turbine with GP regression fit of noise free observations with the two standard deviations plotted as shaded area.

Figure 13 shows the results of the turbine's power output and its GP prediction fit of noisy observations. The predicted responses when the signals included noise do not cross the observations, and the prediction intervals become wide. Figure 14 demonstrates the blade pitch angle profile to keep maximum power output, as expected.

Modelling methods of a wind turbine, such as Neural Network, treat the noise and the actual data. In contrast, GP treats the noise as an independent variable, effectively overcoming the randomness and noise problems and establishing an effective model [22].

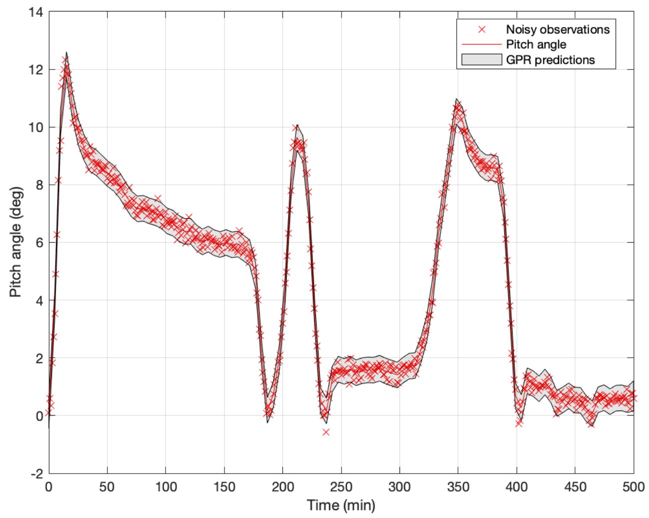

Fig. 13. The power output of turbine with GP regression fit of noisy observations and the two standard deviations plotted as shaded area.

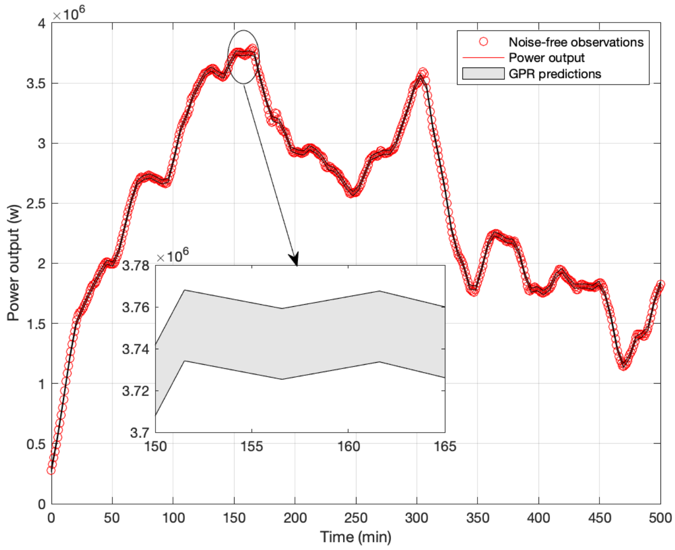

Fig. 14. The control pitch angle with the two standard deviations plotted as shaded area.

8. Conclusions

This article tested the GP regression algorithm under wind speed variation and considered tower shadow and wind shear effects. The application of GPs to wind turbine modelling effectively fits the model and identifies wind shear and tower shadow effects.

The prediction of power wind turbines improves if the wind speed is included, and the fluctuations are assumed to be a function of previous wind speed. The predicted responses when the signals included noise do not cross the observations, and the prediction intervals become wide.

The results show that of the turbine's power output and its GP prediction fit of noisy observations. GP carefully follows the expected variance values of the wind speed. The expected variance is 0.65 and the time elapsed is 0.1425 seconds.

For future work, once we have an accurate wind model, we can design an algorithm to control and optimize the pitch angle of each blade and rotor speed.

Nomenclatures

A	The swept area, m^2
C_p	The aerodynamic coefficient
d	Tower diameter, m^2
f	The frequency rotation of the turbine, Hz
ℓ	Hyperparameter
P_e	The electrical power, W
R	The radius of turbine hub, m
v_{eq}	The equivalent wind speed, m/s
v_{ts}	The tower shadow, m/s
v_{ws}	The wind shear, m/s
w	The angular rotor speed, rps
w_r	The rotor speed, rps

Greek Symbols

β	The blade pitch angle, deg.
ε	Noise $\sim \mathcal{N}(0, \sigma_n^2)$
$\kappa(x, x')$	kernel function
λ	The tip speed ratio
μ	Mean value of the function
ρ	Air density, kg/m^3
σ	Variance value
τ	Time constant, s

References

1. Pandit, R.; and Infield, D. (2018). Gaussian process operational curves for wind turbine condition monitoring. *Energies*, 11(7), 1631.
2. Stetco, A.; Dinmohammadi, F.; Zhao, X.; Robu, V.; Flynn, D.; Barnes, M.; and Nenadic, G. (2019). Machine learning methods for wind turbine condition monitoring: A review. *Renewable Energy*, 133, 620-635.

3. Wang, J.; and Li, Y. (2018). Multi-step ahead wind speed prediction based on optimal feature extraction, long short term memory neural network and error correction strategy. *Applied energy*, 230, 429-443.
4. Erdem, E.; and Shi, J. (2011). ARMA based approaches for forecasting the tuple of wind speed and direction. *Applied Energy*, 88(4), 1405-1414.
5. Mauricio, J.A. (1995). Exact maximum likelihood estimation of stationary vector ARMA models. *Computational Statistics & Data Analysis*, 50(12), 282-3644-3662.
6. Zhang, C.; Wei, H.; Zhao, X.; Liu, T.; and Zhang, K. (2016). A Gaussian process regression based hybrid approach for short-term wind speed prediction. *Energy Conversion and Management*, 126, 1084-1092.
7. Chen, K.; and Yu, J. (2014). Short-term wind speed prediction using an unscented Kalman filter based state-space support vector regression approach. *Applied Energy*, 113, 690-705.
8. Nielsen, H.A.; Madsen, H.; and Nielsen, T.S. (2006). Using quantile regression to extend an existing wind power forecasting system with probabilistic forecasts. *Wind Energy*, 9(1-2), 95-108.
9. Li, G.; and Shi, J. (2010). On comparing three artificial neural networks for wind speed forecasting. *Applied Energy*, 87(7), 2313-2320.
10. Manobel, B.; Sehnke, F.; Lazzús, J.A.; Salfate, I.; Felder, M.; and Montecinos, S. (2018). Wind turbine power curve modeling based on Gaussian processes and artificial neural networks. *Renewable Energy*, 125, 1015-1020.
11. Hoseinzadeh, S.; Sohani, A.; and Heyns, S. (2021). Comprehensive analysis of the effect of air injection on the wake development of an airfoil. *Ocean Engineering*, 220, 108455.
12. Strutz, T. (2010). *Data fitting and uncertainty*. A practical introduction to weighted least squares and beyond. Vieweg+ Teubner.
13. Marchetti, A.G.; François, G.; Faulwasser, T.; and Bonvin, D. (2016). Modifier adaptation for real-time optimization—methods and applications. *Processes*, 4(4), 55.
14. Cai, H.; Jia, X.; Feng, J.; Li, W.; Hsu, Y.-M.; and Lee, J. (2020). Gaussian process regression for numerical wind speed prediction enhancement. *Renewable Energy*, 146, 2112-2123.
15. Carrillo, C.; Montaño, A.F.O.; Cidrás, J.; and Díaz-Dorado, E. (2013). Review of power curve modelling for wind turbines. *Renewable and Sustainable Energy Reviews*, 21, 572-581.
16. Dolan, D.S.L.; and Lehn, P.W. (2006). Simulation model of wind turbine 3p torque oscillations due to wind shear and tower shadow. *IEEE Transactions on energy conversion*, 21(3), 717-724.
17. Virgolino, G.C.M.; Mattos, C.L.C.; Magalhães, J.A.F.; and Barreto, G.A. (202). Gaussian processes with logistic mean function for modeling wind turbine power curves. *Renewable Energy*, 162, 458-465.
18. Hoseinzadeh, S.; Bahrami, A.; Mirhosseini, S.M.; Sohani, A.; and Heyns, S. (2020). A detailed experimental airfoil performance investigation using an equipped wind tunnel. *Flow Measurement and Instrumentation*, 72, 101717.

19. Ragheb, M.; and Ragheb, A.M. (2011). Wind turbines theory-the betz equation and optimal rotor tip speed ratio. *Fundamental and Advanced Topics in Wind Power*, 1(1), 19-38.
20. Blaabjerg, F.; Xu, D.; Chen, W.; and Zhu, N. (2018). Advanced control of doubly fed induction generator for wind power systems. *John Wiley and Sons*.
21. Bharani, R.; and Sivaprakasam, A. (2019). A large volume wind data for renewable energy applications. *Data in Brief*, 25, 104291.
22. Zhou, J.; Guo, P.; and Wang, X.-R. (2014) Modeling of wind turbine power curve based on Gaussian process. *Proceedings of the 2014 International Conference on Machine Learning and Cybernetics*. Lanzhou, 71-76.